J. Am. Soc. Mass Spectrom. (2016) 27:1383–1392
DOI: 10.1007/s13361-016-1411-3

RESEARCH ARTICLE

Microhydration of Deprotonated Nucleobases

Henryk Wincel

Institute of Physical Chemistry, Polish Academy of Sciences, 01-224, Warsaw, Poland

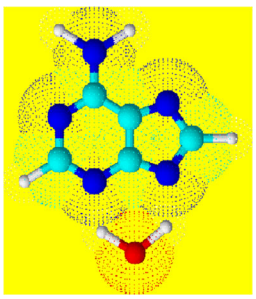

Abstract. Hydration reactions of deprotonated nucleobases (uracil, thymine, 5-fluorouracil,2-thiouracil, cytosine, adenine, and hypoxanthine) produced by electrospray have been experimentally studied in the gas phase at 10 mbar using a pulsed ion-beam high-pressure mass spectrometer. The thermochemical data, ΔH^o, ΔS^o, and ΔG^o, for the monohydrated systems were determined. The hydration enthalpies were found to be similar for all studied systems and varied between 39.4 and 44.8 kJ/mol. A linear correlation was found between water binding energies in the hydrated complexes and the corresponding acidities of the most acidic site of nucleobases. The structural and energetic aspects of the precursors for the hydrated complexes are discussed in conjunction with available literature data.

Keywords: Hydration energies, Deprotonated nucleobases, High-pressure mass spectrometry

Received: 6 January 2016/Revised: 17 April 2016/Accepted: 19 April 2016/Published Online: 13 May 2016

Introduction

Hydrogen bonding plays a central role in biological structures and function, including protein and nucleic acid folding, molecular recognition, signal transduction, and enzymatic catalysis [1]. Hydrogen bonds in DNA and the interaction between two complementary nucleobases, which are held together by NH–O and NH–N hydrogen bonds, are dependent on the intrinsic basicity of the acceptor atoms as well as on the acidity of the donor groups [2, 3]. The strength of these bonds is related to the p*K*a values of the components [4]. The hydrogen bonding between the nucleobases (NB) in DNA and RNA duplexes is very important for a greater understanding of their structure and function in vivo [5].

When ionizing radiation interacts with living organisms, the low-energy electrons (<15 eV) efficiently damage DNA by inducing single- and double-strand breaks [6]. These alterations are initiated by dissociative electron attachment (DEA) with the initial capture of an electron leading to a temporary negative ion, which may decompose by spontaneous ejection of the electron or by dissociation into neutral and anionic fragments [6, 7]. Gas- phase studies have shown that the most abundant fragment anions formed via the DEA process of uracil [8], thymine [9, 10], cytosine [11], 2-thiouracil [12], adenine [13], and hypoxanthine [14] are the deprotonated nucleobases $[NB\text{-}H]^-$. The formation of these anions is energetically driven by the electron affinity of the $[NB\text{-}H]^{\bullet}$ radicals, which lie in the range between 3 and 4.5 eV [9, 11, 15, 16].

A large amount of computational [17–42] and experimental [20, 27, 31, 32, 36–39] investigations has been carried out in order to determine the acidities of nucleobases. Several of these studies were focused on the examination of the properties of deprotonated uracil and its derivatives [17, 18, 20–22, 24, 26–31, 35–37, 39, 40, 42], cytosine [23, 28, 34, 37, 39], adenine and its derivatives [19, 32, 33, 37, 41], hypoxanthine [38], and guanine [41] in the context of the mechanism of action of the enzymes, which recognize damaged bases and remove them from DNA. For example, the mechanism for uracil excision from the genome by the enzyme uracil DNA glycosylase (UDG) involves nucleophilic attack by some form of activated water of the *N*-glycosidic bond connecting the nucleobase to the sugar and formation of $N1^-$ deprotonated uracil as the leaving group [43, 44].

Although it is essential to characterize the properties of deprotonated forms of isolated nucleobases, it is equally important to examine their properties in environments that mimic some of the aspects of the biological world. Water is the natural medium of biological systems, and for that reason our investigations are focused on the hydration of different ionic forms of nucleobases. In our previous studies, we investigated the thermochemical properties for the gas-phase hydration of protonated nucleobases and protonated nucleosides [45], sodiated and potassiated nucleobases [46], and protonated and sodiated thiouracils [47].

In this paper, we present the experimental investigations of the interactions of one molecule of water with deprotonated uracil [**U**-H]$^-$, thymine [**T**-H]$^-$, 5-fluorouracil [5F**U**-H]$^-$, 2-thiouracil [2S**U**-H]$^-$, cytosine [**C**-H]$^-$, adenine [**A**-H]$^-$, and hypoxanthine [**H**-H]. Schemetic structures and atom labeling of neutral nucleobases are shown in Scheme 1.

Correspondence to: Henryk Wincel; *e-mail:* wincel@ichf.edu.pl

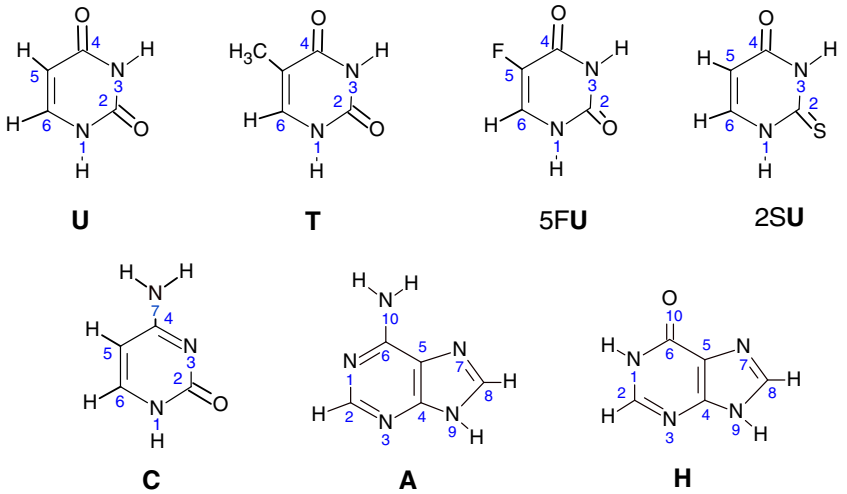

Scheme 1. Structures and atom numbering of the systems considered in the present study

The five nucleobases (**U**, **T**, **C**, **A**, and **G**) are directly involved in the formation and the stability of the well-known double helix structure of DNA and RNA. We could not conduct measurements with **G** (guanine) as it is sparingly soluble in the electrospraying solution. **H** is a mutagenic purine base that most commonly arises from the oxidative deamination of **A**, and is associated with carcinogenesis and cell death [38]. Modified nucleobases, 5-F**U** and 2S**U**, are important and interesting compounds because of their biological and pharmacological properties. 5-F**U** is widely used in the treatment of a range of cancers, including colorectal and breast cancers, and cancers of aerodigestive tract [48, 49]. 2-S**U** has found medical applications as antithyroid and anticancer drugs [50–52].

Several theoretical studies on the interaction of deprotonated nucleobases with water have been performed. Kryachko et al. [22] estimated the binding energies of water molecule with the $N3^-$ anions of 2-S**U**, 4-S**U**, and 2,4-dS**U**. Wetmore and coworkers [29, 30] computationally investigated the binding energies of neutral and the $N1^-$ anionic uracil and its derivatives with small molecules (NH_3, H_2O, or HF) at the O_2(N3), O_4(N3), and O_4(C5) binding positions. Their results showed that the binding strengths are relatively independent of the substituent. Furthermore, they reveal decrease in the deprotonation energy at N1 by about 20 kJ/mol with one associated water to uracil [29]. Computational studies by Bachrach and Dzierlenga [42] have indicated that the difference (54.4 kJ/mol) in deprotonation energy between the N1 and N3 sites of uracil decreases with each added water up to four. At this point, the energy difference has been halved, but addition of a fifth or sixth water has little effect on the energy difference. The Wetmore group [34] carried out density functional theory studies of the complexes between NH_3, H_2O, or HF molecules and four main binding sites in neutral and N1 deprotonated cytosine. They found that the trends in the effects of hydrogen bonds on the N1 acidity are similar for all pyrimidines. To the best of our knowledge, no experimental results on the gas-phase hydration of deprotonated nucleobases have been reported.

Experimental

The experiments were performed with a high-pressure mass spectrometer using a pulsed ion-beam ESI ion source, which has been described in detail elsewhere [53]. Briefly, the reactant ions were produced by electrospraying water/acetonitrile (20%:80%) solutions containing ~2.0 mM nucleobase to which a few drops of ammonium hydroxide were added. The pH value of solution measured with Schott CG 837 (Mainz, Germany) instrument was ~10.5. Each solution was supplied to a silica capillary (15 μm i.d., 150 μm o.d) by a syringe pump at a rate of 0.8 μL/min, and a negative voltage was held at approximately 4 kV.

The clustered ions were desolvated by a dry nitrogen gas counter current and in a heated (~80°C) pressure-reducing capillary through which they were introduced into the forechamber, and then deflected toward a 3-mm orifice in the interface plate leading to the reaction chamber (RC). Ions drifting across the RC toward the exit slit under the influence of a weak electric field (2 V/cm at 10 mbar) were hydrated and reached equilibrium prior to being sampled to the mass analysis section of the mass spectrometer. Ion detection was provided by a channeltron equipped with a conversion dynode. The output pulses of the multiplier were counted using a multichannel scaler with dwell-time per channel of 1 μs. Mass spectra were registered with continuous ion sampling, while for equilibrium determination the ion beam was injected into the RC in a pulsing mode by applying short pulses (–52 V, 200 μs) to the deflection electrode. The latter mode of operation allows for measurements of the arrival time distribution (ATD) of the ions across the RC.

The reagent gas mixture consisting of pure N_2 as the carrier gas at about 10 mbar and a known partial pressure of water vapor (0.1–0.25 mbar) was supplied to the RC via the heated reactant gas inlet (RGI) at a flow rate of ~100 mL/min. The pressure was measured with an MKS capacitance manometer attached near the inlet of the RGI. The amount of water

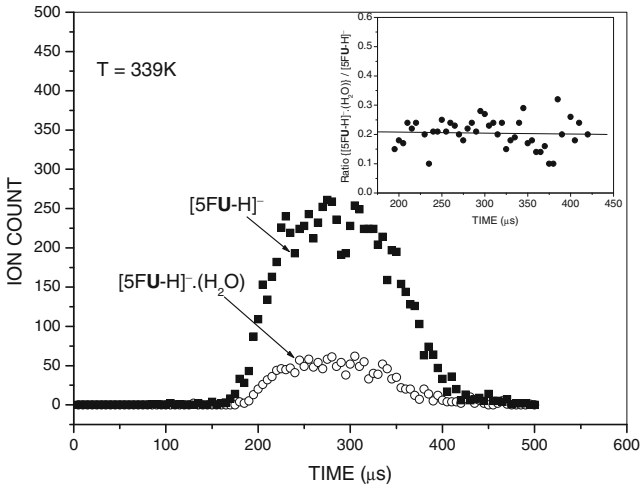

Figure 1. Arrival time distributions of the reactant, $[5FU\text{-}H]^-$, and product, $[5FU\text{-}H]^-\cdot(H_2O)$, ions. The inset shows the ratio of ion intensities,$\{[5FU\text{-}H]^-\cdot(H_2O)\}/[5FU\text{-}H]^-$ as a function of ion residence time

introduced into the N_2 gas flow was kept constant throughout the temperature-dependent measurements of the equilibrium constants. Water concentrations were controlled continuously with a calibrated temperature and humidity transmitter (Delta OHM, Type DO 9861T; Casselle di Selazzano, Italy). The RC temperature was monitored by an iron-constantan thermocouple, which was embedded close to the ion exit slit; the temperature can be varied from ambient to ~300°C by electrical heaters.

The chemicals, N_2 (Polish product, 99.999%) and the nucleobase samples: uracil, thymine, cytosine, adenine, and hypoxanthine obtained from Aldrich Chemical Co. (Steinheim, Germany), 2-thiouracil from Alfa Aesar GmbH & Co. KG (Karlsruhe, Germany), and 5-fluorouracil from abcr GmbH & Co. KG (Karlsruhe, Germany) were used without further purification. The water was deionized with a Millipore purifier, type Elix 5 (Vienna, Austria).

The gas-phase hydration energies of deprotonated nucleobases were determined by measurement of the equilibria described by the general reaction (1)

$$[\text{NB-H}]^- \cdot (H_2O)_{n-1} + H_2O \leftrightarrow [\text{NB-H}]^- \cdot (H_2O)_n \quad (1)$$

for which the thermodynamic equilibrium constant is

$$K_{n-1,n} = \left(I_n \cdot P_o \middle/ I_{n-1} \cdot P\right) \quad (2)$$

where I_n and I_{n-1} are recorded ATD peak areas of $[\text{NB-H}]^-\cdot(H_2O)_n$ and $[\text{NB-H}]^-\cdot(H_2O)_{n-1}$ respectively, and P is the known partial pressure of water (in mbar). The standard pressure P_o is 1000 mbar. Equilibrium attainment in the RC was verified by comparing the ATDs of the reactant and product ions, and testing that the I_n /I_{n-1} ratio was independent of ion residence time. A typical example of such tests is shown in Figure 1 for the (0,1) hydration step of $[5FU\text{-}H]^-$. The inset of the figure shows that within the error limits and the limits of statistical noise, the ratio $\{[5FU\text{-}H]^-\cdot(H_2O)\}/[5FU\text{-}H]^-$ remains essentially constant, suggesting the attainment of equilibrium for the system.

Measuring $K_{n-1,n}$ as a function of temperature T and using the thermodynamic relationships (3) and (4)

$$\ln K_{n-1,n} = \left(\Delta S^o{}_n \middle/ R\right) - \left(\Delta H^o{}_n \middle/ RT\right) \quad (3)$$

$$\Delta G^o{}_n = \Delta H^o{}_n - T\Delta S^o{}_n \quad (4)$$

Table 1. Experimental Enthalpies, Entropies, and Free Energy Values[a] for the Hydration of Deprotonated Nucleobases[a]

Ion	$-\Delta H^o{}_n$ (kJ/mol)	$-\Delta S^o{}_n$ (J/mol K)	$-\Delta G^o{}_n$ (kJ/mol)[b]	Acidity (kJ/mol)	
$[2SU - H]^-$	39.7(2); *46.5*[c]	67.4(10)	19.7(6)	1365.3[d] (N1)	1411.6[d] (N3)
$[5FU - H]^-$	40.6(2); *41.9*[e]	65.3(5)	21.1(4)	1376.5[f] (N1)	1435.1[f] (N3)
$[U - H]^-$	43.0(2); *42.6*[e]	64.4(7)	24.0(4)	1393.3[f,g,h] (N1)	1451.8[f,g] (N3)
$[T - H]^-$	43.5(2); *43.3*[e]	71.1(8)	22.5(4)	1401.6[i] (N1)	1447.7[i] (N3)
$[C - H]^-$	44.8(2)	70.3(6)	23.8(4)	1422.6[f] (N1)	1447.7[f] (N7)
$[A - H]^-$	42.7(2)	68.2(5)	22.7(4)	1393.3[f,j](N9)	1472.7[f,j] (N10)
$[H - H]^-$	42.2(2)	63.0(6)	23.4(4)	1389.1[k](N9)	1539.7[k]
J^-	42.0(2)	68.2(8)	21.7(4)		
	42.3[l]	66.1[l]	22.6[l]		

Standard pressure is 1000 mbar.
[a] Uncertainties in parentheses.
[b] $-\Delta G^o{}_n$ at 298 K.
[c] Calculated water binding energy for the N3 anionic complex of $[2SU - H]^-\bullet(H_2O)$, configuration **1c**, Ref. [22].
[d] Ref. [35].
[e] Calculated water binding energy for the $[NB - H]^-\bullet(H_2O)$ complex deprotonated at N1, configuration **1b**, Ref. [30].
[f] Ref. [37].
[g] Ref. [20].
[h] Ref. [31].
[i] Ref. [39].
[j] Ref. [32].
[k] Ref. [38].
[l] Ref. [54].

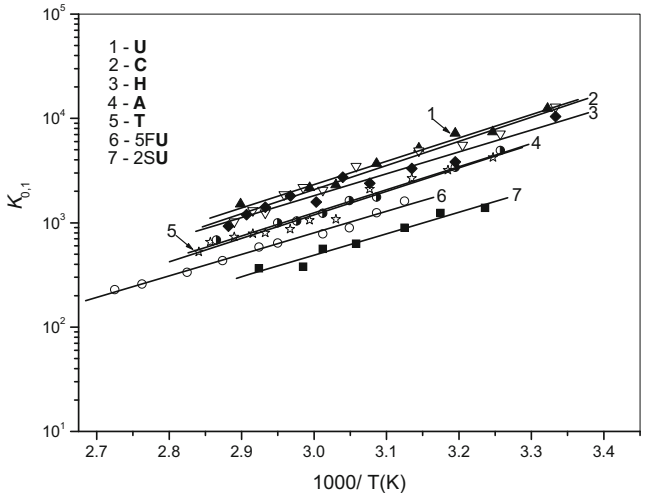

Figure 2. van't Hoff plots of equilibrium constants for the gas-phase reactions: [**NB**-H]$^-$ + H_2O ↔ [**NB**-H]$^-$ ·(H_2O). Compounds **NB** are given in the figure

the values for the enthalpy, ΔH^o_n , entropy, ΔS^o_n , and free energy, ΔG^o_n , of Reaction 1 were obtained. The weighted least-squares fitting procedure was used to obtain the slopes and intercepts of each line. The slopes determine the enthalpy change (ΔH^o_n) and the intercepts yield the corresponding ΔS^o_n value. The uncertainty corresponds to the standard deviation of the linear least-squires fit.

During these experiments, we determined thermochemical data for the hydration Reaction 5 to support the validity of the present results and provide bases for comparison with the data obtained in previous studies [54] (see Table 1).

$$J^- + H_2O \leftrightarrow J^-(H_2O) \quad (5)$$

Results and Discussion

The van't Hoff plots for the temperature studies of the hydration reactions of [NB-H]$^-$ are shown in Figure 2 and the results are summarized in Table 1, along with related literature data. The results show that the hydration enthalpies, ΔH^o, for all anions are essentially the same, and the small differences can be attributed to the correlation with the gas-phase acidities of nucleobases. The data will be presented elsewhere. In this work, the term "gas-phase acidity" is used to refer to the enthalpy change, ΔH^o_{ac}, associated with deprotonation. Table 1 shows the gas-phase acidities of the most acidic and the less acidic site of nucleobases. For all these nucleobases, more than one site in the molecule can be deprotonated. Similarly to the neutral nucleobases, their deprotonated forms can exist in several tautomeric structures, and the measured hydration enthalpy changes for [NB-H]$^-$ may represent an average over several contributing structures. The formation of [NB-H]$^-$ by ESI could occur from different locations. The anions produced from aqueous solution may be different from those formed in the gas-phase region, in which changes can occur either in the transition of the ion from the charged droplet to the gas phase or in the gas phase due to ion-molecule reactions [55], where catalyzed isomerization can occur in the presence of neutral nucleobase [20]. The possible anionic structures of [NB-H]$^-$ created by ESI that might be involved in the hydration equilibrium 1 are characterized in the following discussion.

Uracil and Its Derivatives

For uracil and its derivatives, the possible deprotonation sites are N1 and N3. In the gas phase, N1 is more acidic than N3, by about 45–60 kJ/mol (see Table 1), while in aqueous solution the N1 and N3 acidities of uracil are indistinguishable, and the N1$^-$ monoanion is in equilibrium with that of N3$^-$ in ca. 1:1 ratio [43]. A similar proportion also holds for the mixtures of the monoanions N1$^-$ and N3$^-$ in aqueous medium of thymine [56] and 2-thiouracil [57]. For 5-fluorouracil, the spectral data [58] show the predominance of N3$^-$ in the N1$^-$ and N3$^-$ monoanionic mixture in aqueous solution. However, in alkaline aqueous solution, the situation can be different. Theoretical studies [59] show that in alkaline aqueous media, the deprotonation at N1, with equilibrium constant, $K_{eq}^{(N1)}$, should be the dominant path of uracil ionization. This result is supported by the reaction field calculations with the isodensity polarizable continuum (IPC) model, with the equilibrium constant ratio, $K_{eq}^{(N1)}/ K_{eq}^{(N3)} = 5 \times 10^4$. In the case of 5F**U**, the N1$^-$/ N3$^-$ anion fraction ratio in aqueous alkaline solution was found to be 0.61 [60]. The N3$^-$ anion, if formed in aqueous solution, in the gas phase can isomerize to N1$^-$ in the presence of neutral nucleobase [20]. According to the in vacuo ab initio calculations, the N1$^-$ anion of [**U**-H]$^-$ is more stable than N3$^-$ by 58.5 kJ/mol [59]; for [5F**U**-H]$^-$ this difference is 49.9 kJ/mol [60]. The energy barrier (185.4 kJ/mol) calculated [61] for the uracil N1$^-$ —> N3$^-$ conversion is too high to be overcome at thermal energies in our instrument. Therefore, it is reasonable to assume that the N1$^-$ would be the predominant form of the [NB-H]$^-$ anions of uracil and its derivatives (structure 1 in Scheme 2) formed by ESI in the present study and these species are the most favorable precursors for hydrated complexes. Calculations [42] for the uracil N1$^-$ predict that the most stable complex with water, **1a**, is formed when water is attached to the anion in a bidentate fashion between the deprotonated N1 and the adjacent carbonyl oxygen. Configuration **1b** and the complexes with water binding at the O4(C5) and O4(N3) positions in uracil (not shown in Scheme 2), are significantly (at least 12.6 kJ/mol) higher in energy than **1a** [42] and would be expected to be minor in abundance under the present experiments. It is very likely that the **1a** and **1b** structures are also formed from the hydrated structure **1** of [2S**U**-H]$^-$, [5F**U**-H]$^-$, and [**T** H]$^-$.

As can be seen in Table 1, for the [**U**-H]$^-$, [**T**-H]$^-$, and [5F**U**-H]$^-$ anions, the measured ΔH^o values are very close to the calculated [30] binding strengths between water and the N1$^-$ anions in the O2(N3)–H_2O complex, **1b**, with water bound to the carbonyl oxygen adjacent to N1$^-$. In the case of structure **1c**, the computed [22] binding energy of water (46.5 kJ/mol) to

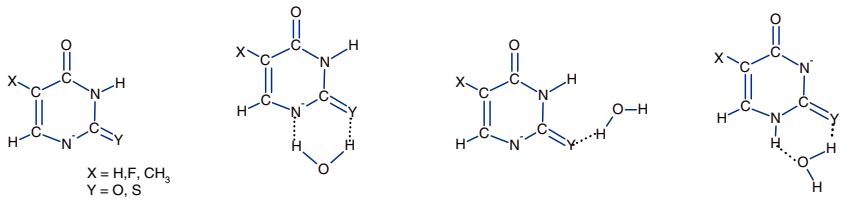

Scheme 2. Structures of deprotonated uracil and its derivatives, and their complexes with water molecule

the $N3^-$ anion of $[2S\mathbf{U}\text{-}H]^-$ is significantly higher than the experimental hydration enthalpy value (39.7 kJ/mol, Table 1). This comparison supports that the $N1^-$ anions of uracil and its derivatives are the dominant precursors for the hydrated complexes of $[NB\text{-}H]^-$ observed under the present experiments.

Cytosine

According to the calculations [39], the canonical tautomer of cytosine, **2**, is the most stable and the three other most stable tautomers are higher in energy by 7.1 (**2a**), 10.5 (**2b**), and 9.2 kJ/mol (**2c**). The next most stable tautomer is predicted to be lying 16.7 kJ/mol higher in energy than **2** (Scheme 3).

As it has been shown [39] that the cytosine formed by electrospray of a methanol aqueous solution adopts predominantly the **2** form, where the most acidic site is N1. Thus, it might be expected that the $N1^-$ anion of the tautomer **2** should be the dominant precursor of the $[\mathbf{C}\text{-}H]^- \cdot (H_2O)$ complex formed in the present experiments. The measured hydration energy for this complex (44.8 ± 2 kJ/mol, Table 1), is significantly lower than the water binding strengths calculated for the **2e** (57.1 kJ/mol) and **2f** (51.1 kJ/mol) complexes [34].These results imply that the **2d** complex dominates in the equilibrium reaction 1.

Adenine

In the gas phase, the canonical tautomer of adenine, **3**, is the most stable and predominant species. The next two tautomers, **3a** and **3b**, are higher in energy by ~34 kJ/mol [41, 62], Scheme 4.

Tautomerization **3** —> **3a** and **3** —> **3b** is predicted [63] to occur with a very large activation barrier (250–293 kJ/mol), indicating that the processes may not occur in the gas phase. In water, however, the energy difference between the canonical and these two tautomers is reduced to 4.7 kJ/mol (**3a**) and 18.0 kJ/mol (**3b**) [64]. The experimental measurements [65–67] and calculations [68] show that only the **3** and **3a** tautomers might be present in an aqueous solutions, and their population ratio, **3/3a**, was estimated to be in the range of 3.6–4.9 at 293 K.

In our experiments, the formation of $[\mathbf{A}\text{-}H]^-$ by ESI can occur from different locations of the parent molecule. In aqueous solution, these anions may result from the dominant tautomer **3** with possibly up to 20% of the **3a** tautomer. In the atmospheric pressure region, the ion formation predominantly from **3** may be expected. Therefore, it is very likely that the **3c** anion (Scheme 4) formed from a mixture of **3** and **3a** should be the precursor for the hydrated complexes.

The negative Mulliken charges predicted by theoretical studies [69] for the N atoms of the adenine $N9^-$ are equal to 0.25e (N1), 0.25e (N3), 0.23e (N9), 0.23e (N7), and 0.20e (N10). These results suggest that the negative charge in **3c** is uniformly distributed, and a possibility exists that the resonance structures of this anion, **3d**, **3e**, **3f**, and **3 g**, can interact with the water molecule leading to the hydrated complexes **3 h**, **3i**, and **3j** (Scheme 4). It is also possible that we have a mixture of these complexes, and the hydration energies measured for these systems represent an average of their contribution. However, a comparison of the calculated [33] gas-phase acidities for

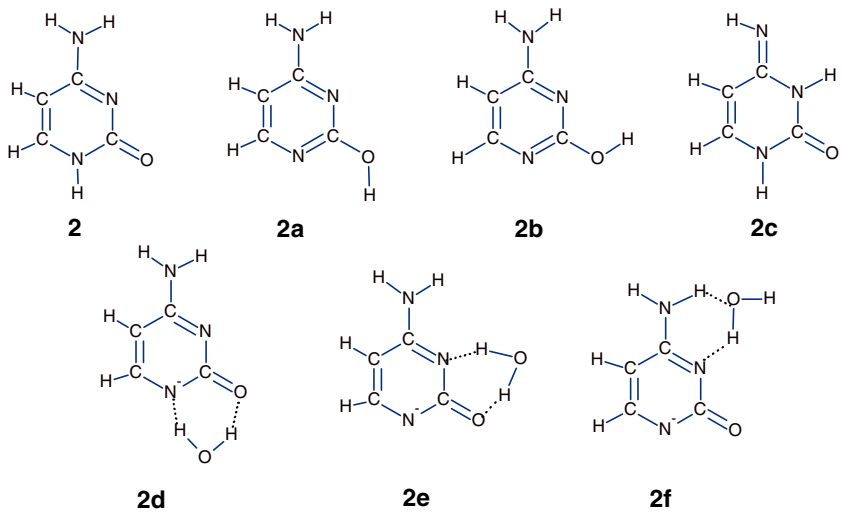

Scheme 3. Structures of four tautomers of cytosine and their deprotonated complexes with water

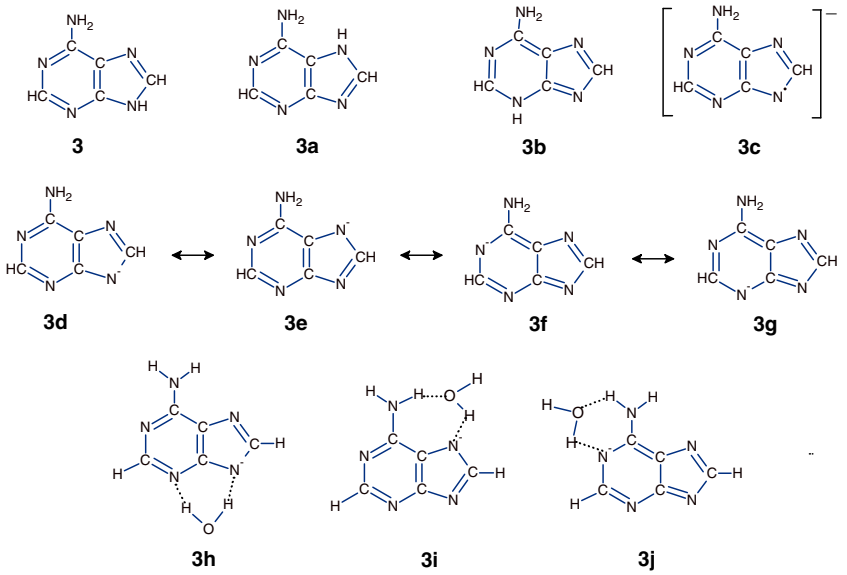

Scheme 4. The three most stable tautomers of adenine (**3**, **3a**, and **3b**) and the resonance structures for deprotonated adenine (**3d**, **3e**, **3f**, and **3 g**), and their hydrated complexes (**3 g**, **3 h**, and **3i**)

the adenine N9H (334.8 kJ/mol), N7H (326.7 kJ/mol), N3H (326.7 kJ/mol), and N1H (316.3 kJ/mol) with the measured [32] acidity of the most acidic site N9H (333 ± 2 kJ/mol) may imply the predominant formation of the **3 h** complex.

Hypoxanthine

Theoretical and experimental studies [38, 70–72] indicate that in the gas phase hypoxanthine can exist mainly in two keto tautomeric forms, **4** and **4a**, (Scheme 5). The canonical structure **4** is calculated to be less stable than the **4a** by 3.5 kJ/mol; the next most stable tautomer, **4b**, is 22.6 kJ/mol higher in energy than **4a** [38].

The calculations [70] show that the **4a** tautomer represents about 80% of the population in the gas phase. The predicted concentration for **4b** would be less than 0.1%. Hydration shifts in the tautomeric equilibria toward the **4** form; in the case of the dihydrated species, the populations of the **4** and **4a** tautomers would be about 50% [70]. Also, quantum chemical and Monte-Carlo calculations [73] indicate that both species might be coexisting under similar tautomeric populations in neutral hypoxanthine aqueous solution. The resonance Raman spectroscopy and quantum chemical calculations study [74] reported that in solution the hypoxanthine anion is formed only via deprotonation of the N7H and N9H sites. Thus, based on these results, one may assume that [**H**-H]$^-$ formed from **4** and **4a** by ESI, either in solution or within the droplets, represent a mixture of the deprotonated tautomers of similar populations. The negative Mulliken charge distribution predicted by the calculations [74] for the N3, N7, N9, and O10 atoms of the **4c** anion are equal to 0.509, 0.543, 0.541, and 0.589e, respectively. The charges at the N3 and N9 atoms are comparable with those of N7 and O10, and both these positions could be the reactive sites for water interaction with resonance structures **4d** and **4e** leading to the complexes **4f** and **4g**, as schematically depicted in Scheme 5. The acidity values calculated [38] for the most

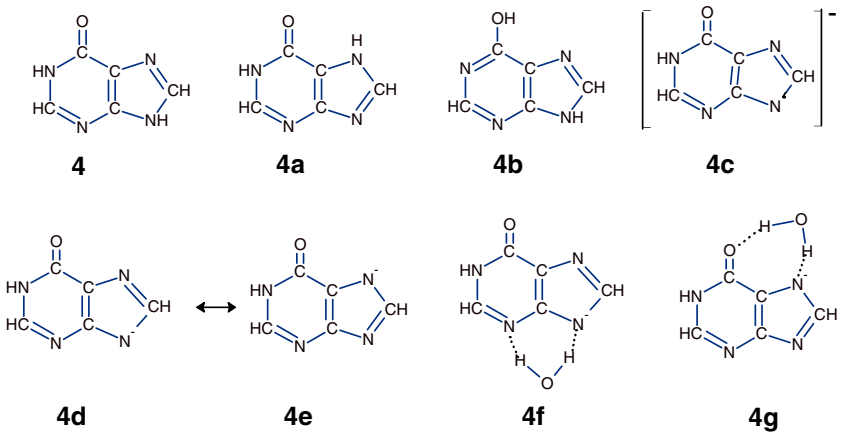

Scheme 5. Most stable tautomers of hypoxanthine (**4**, **4a**, and **4b**), and the resonance structures for deprotonated hypoxanthine (**4d** and **4e**) and their hydrated complexes (**4f** and **4 g**

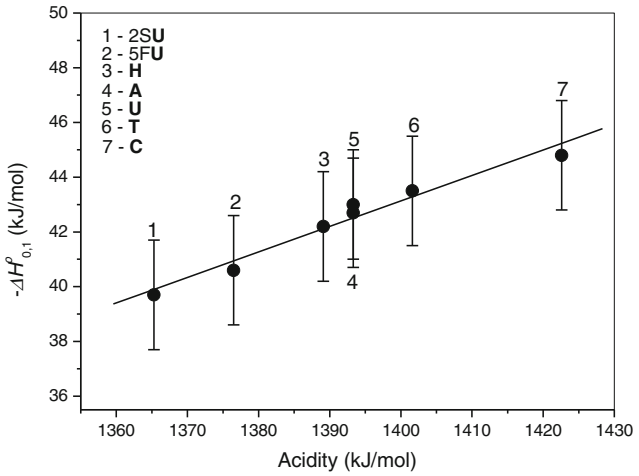

Figure 3. Plot of the binding energies, $-\Delta H^{o}_{0,1}$, versus corresponding acidity of the most acidic site of nucleobases. The acidity values are given in Table 1

acidic sites, N9H in **4** (1383.8 kJ/mol) and N7H in **4a** (1386.2 kJ/mol), are consistent with the measured value (1389.1 ± 8 kJ/mol).

Correlation Between Water Binding Energies and Acidities

A plot of the binding energies ($-\Delta H^{o}$) of water molecule in the $[NB\text{-}H]^{-}\cdot(H_2O)$ complexes versus the corresponding gas phase acidities of the most acidic site of NB is shown in Figure 3. The gas-phase acidity values used for this figure and also quoted in Table 1, except for 2S**U** [35], are obtained experimentally and reported in the literature [20, 31, 37–39]. A

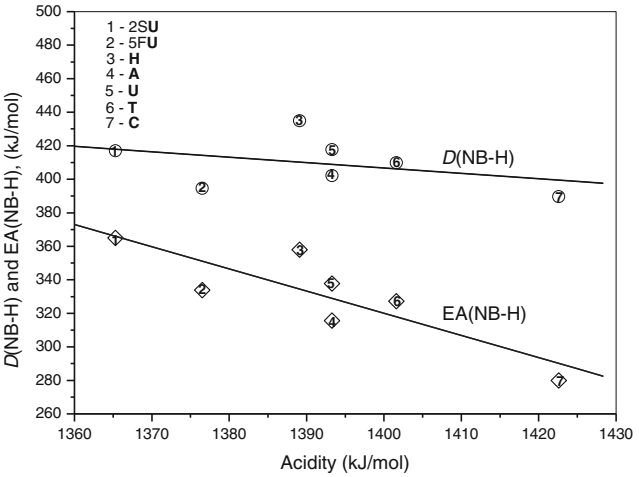

Figure 4. Plot of the N–H bond dissociation energies of **NB**, *D*(**NB**-H), and the electron electron affinities of the (**NB**-H) radical, EA(**NB**-H), versus corresponding acidity of the most acidic site of nucleobases. The acidity values are given in Table 1. The *D*(**NB**-H) and EA(**NB**-H) values for 5F**U**, **A**,**U**,**T**, and **C** are taken from Ref. [37]; for **H**, Ref. [14]. For 2S**U**, the EA(**NB**-H)=365 kJ/mol was estimated as the difference of *D*(NB-H) – E(DEA) based on E(DEA)=52.9 kJ/mol [12] and using for *D*(NB-H) the same value as for **U**

fair linear relation is observed in Figure 3. The correlation coefficient is 0.98. Changes in hydration enthalpies of $[NB\text{-}H]^{-}$ can be thermochemically analyzed on the basis of the gas-phase acidity enthalpy, ΔH^{o}_{ac}, for deprotonation given by Equation (6)

$$\Delta H^{o}_{ac} = D(\text{NB-H}) - \text{EA}(\text{NB-H}) + \text{IE}(\text{H}) \quad (6)$$

where *D*(NB–H) represents the bond energy for N–H broken during deprotonation of NB, EA(NB–H) the electron affinity of the [NB-H] radical, and IE(H) the ionization energy of the H atom. Since the IE(H) is constant, the ΔH^{o}_{ac} should be dependent on the *D*(NB-H) – EA(NB-H) difference, which is related to the energy for dissociative thermal electron attachment by E(DEA) = *D*(NB-H) – EA(NB-H). For the systems studied, the approximate correlations in Figure 4 show that the EA(NB–H) values undergo larger change than those of *D*(NB-H). The slopes ratio of EA(NB-H)/*D*(NB-H) is equal to about 4. This implies that the electron affinity of the [NB-H] radical is the major factor determining the magnitude of the binding energy of water in the $[NB\text{-}H]^{-}\cdot(H_2O)$ complexes, which is largely due to electrostatic attraction.

Comparison to Neutral and Protonated Nucleobase

The hydration enthalpies obtained in this work for $[NB\text{-}H]^{-}\cdot(H_2O)$ along with the literature values calculated [19, 26, 67, 72] for the neutral, $[NB]\cdot(H_2O)$, and those measured [45] previously for protonated forms, $[NB+H]^{+}\cdot(H_2O)$, using the same methods employed here are compared in Table 2 and Figure 5. For all anionic complexes, the water binding energies are larger than those for the corresponding neutral complexes. This confirms the electrostatic nature of water interaction with the anionic forms of nucleobases. The stronger H-bonding interactions in the cationic complexes than those in anionic

Table 2. Binding Energies (kJ/mol) of Water for the Monohydrated

NB	$[NB]\cdot(H_2O)$	$[NB-H]^{-}\cdot(H_2O)$	$[NB+H]^{+}\cdot(H_2O)$
2S**U**	32.2[a,d]	39.7	51.0
5F**U**	34.3[a,e]	40.6	
U	32.7[a,f]	43.0	51.9
T	32.2[a,f]	43.5	54.4
C	37.2[a,f]	44.8	
A	33.6[b,f]	42.7	54.8
H	34.1[c,g]	42.2	52.7

Complexes of Neutral, Deprotonated, and Protonated Nucleobases
[a] In the $[NB]\cdot(H_2O)$ complexes, the water molecule is attached to the N1H bond and the O2(or S2) atom of NB.
[b] Complex formed between the N3 atom and the N9H bond of the canonical tautomer.
[c] Complex formed between the N1H bond and the O10 atom of the keto-N9H tautomer.
The binding energies taken from:
[d] Ref. [75].
[e] Ref. [26].
[f] Ref.[19].
[g] Ref. [70].
The values for $[NB–H]^{-}\cdot(H_2O)$, present work.
The values for $[NB+H]^{+}\cdot(H_2O)$, Ref. [45].

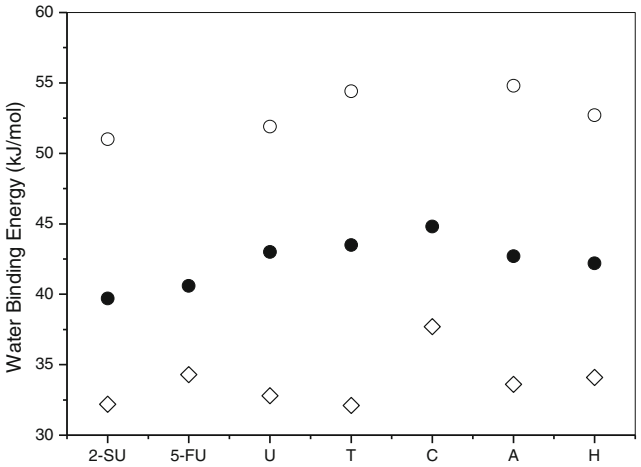

Figure 5. Comparison of the water binding energies for the neutral, NB·(H_2O), (◦); deprotonated, $[NB - H]^-$·(H_2O), (•); and protonated , $[NB+H]^+$·(H_2O), (o), complexes. The binding energy values are given in Table 2

can be attributed to higher positive charge density concentrated on the site of $[NB+H]^+$ protonation compared with a delocalized negative charge in the anionic nucleobases. For example, in the $N1^-$ anions of [**U**-H] $^-$ and [2S**U**-H] $^-$, the large negative charge is located on the O2(S2) and O4 atoms [22, 42]. In [**A**-H] $^-$ and [**H**-H] $^-$, as discussed above, the negative charge is uniformly distributed on the N atoms. The electrostatic potentials calculated [76] for the deprotonated **A**, C, and **T** indicate that the negative charge is "spread" throughout the $[\mathbf{A}\text{-H}]^-$ anion, whereas in $[\mathbf{C}\text{-H}]^-$ the most of the negative charge resides in the C2=O region. The $[\mathbf{T}\text{-H}]^-$electrostatic potential is less delocalized than $[\mathbf{A}\text{-H}]^-$, but more than $[\mathbf{C}\text{-H}]^-$.

Conclusions

In the present work, we have investigated the monohydration of deprotonated nucleobases produced by electrospray from alkaline solutions (pH ~10.5). The results from these experiments suggest that the pyrimidine nucleobases deprotonated at the N1 site are the dominant precursors for the hydrated complexes, $[NB\text{-H}]^-\cdot(H_2O)$. In these systems, the water is most likely involved in a bidentate interaction with deprotonated nitrogen atom $N1^-$ and the O2 (or S2) atom of the adjacent group. The measured hydration enthalpies for $[\mathbf{U}\text{-H}]^-$, $[\mathbf{T}\text{-H}]^-$, and $[5F\mathbf{U}\text{-H}]^-$ are very similar to the binding strengths calculated [30] for the corresponding hydrated complexes with water at the O2(N3) binding position. In the case of adenine and hypoxanthine, the $[\mathbf{A}\text{-H}]^-$ and $[\mathbf{H}\text{-H}]^-$ anions formed by deprotonation of the N9H and N7H tautomers are the precursors for the hydrated complexes, which for both systems most likely represent the mixtures of isomeric structures. The thermochemical properties found for the hydration reactions of $[NB\text{-H}]^-$ are similar within experimental uncertainty. A correlation between the hydration enthalpies and the corresponding acidities of the most acidic site of nucleobases is observed.

Open Access

References

1. Jeffrey, G.A., Saenger, W.: Hydrogen Bonding in Biological Structures. Springer-Verlag, Berlin (1991)
2. Horowitz, S., Trievel, R.C.: Carbon-oxygen hydrogen bonding in biological structure and function. J. Biol. Chem. **287**, 41576–41582 (2012)
3. Lee, J.K.: Insights into nucleic acid reactivity through gas-phase experimental and computational studies. Int. J. Mass Spectrom. **240**, 261–272 (2005)
4. Chen, J., McAllister, M.A., Lee, J.K., Houk, K.N.: Short, strong hydrogen bonds in the gas phase and in solution: theoretical exploration of pKa matching and environmental effects on the strengths of hydrogen bonds and their potential roles in enzymatic catalysis. J. Org. Chem. **63**, 4611–4619 (1998)
5. Lehninger, W.H.: Principles of Biochemistry, 4th edn. Freeman and Company, New York (2005)
6. Boudaïffa, B., Cloutier, P., Hunting, D., Huels, M.A., Sanche, L.: Resonant formation of DNA strand breaks by low-energy (3 to 20 eV) electrons. Science **287**, 1658–1660 (2000)
7. Sanche, L.: Nanoscopic aspects of radiobiological damage: fragmentation induced by secondary low-energy electrons. Mass Spectrom. Rev. **21**, 349–369 (2002)
8. Denifl, S., Ptasińska, S., Hanel, G., Gstir, B., Probst, M., Scheier, P., Märk, T.D.: Electron attachment to gas-phase uracil. J. Chem. Phys. **120**, 6557–6565 (2004)
9. Ptasińska, S., Denifl, S., Mróz, B., Probst, M., Grill, V., Illenberger, E., Scheier, P., Märk, T.D.: Bond selective dissociative electron attachment to thymine. J. Phys. Chem. **123**, 124302-1–124302-7 (2005)
10. Ptasińska, S., Denifl, S., Grill, V., Märk, T.D., Scheier, P., Gohlke, S., Huels, M., Illenberger, E.: Bond-selective H-ion abstraction from thymine. Angew. Chem. Int. Ed. **44**, 1647–1650 (2005)
11. Denifl, S., Ptasińska, S., Probst, M., Hrušák, J., Scheier, P., Märk, T.D.: Electron attachment to the gas-phase DNA bases cytosine and thymine. J. Phys. Chem. A **108**, 6562–6569 (2004)
12. Kopyra, J., Abdout-Carima, H., Kossoski, F., Varella, M.T.: Electron driver reactions in sulphur containing analogues of uracil: the case 2-SU. Phys. Chem. Chem. Phys. **16**, 25054–25061 (2014)
13. Huber, D., Beikircher, M., Denifl, S., Zappa, F., Matejcik, S., Bacher, A., Grill, V., Märk, T.D., Scheierc, P.: High resolution dissociative electron attachment to gas phase adenine. J. Chem. Phys. **125**, 084304-1–084304-7 (2006)
14. Dawley, M.M., Tanzer, K., Carmichael, I., Denifl, S., Ptasińska, S.: Dissociative electron attachment to the gas-phase nucleobase hypoxanthine. J. Chem. Phys. **142**, 215101-1–215101-8 (2015)
15. Parsons, B.F., Sheehan, S.M., Yen, T.A., Neumark, D.M., Wehres, N., Weinkauf, R.: Anion photoelectron imaging of deprotonated thymine and cytosine. Phys. Chem. Chem. Phys. **9**, 3291–3297 (2007)
16. Huang, D.-L., Liu, H.T., Ning, C.-G., Zhu, G.-Z., Wang, L.-S.: Probing the vibrational spectroscopy of the deprotonated thymine radical by photodetachment and state-selective auto-detachment photoelectron spectroscopy via dipole-bound states. Chem. Sci. **6**, 3129–3138 (2015)
17. Nguyen, M.T., Chandra, A.K., Zeegers-Huyskes, T.: Protonation and deprotonation energies of uracil. Implications for the uracil–water complex. J. Chem. Soc. Faraday Trans. **94**, 1277–1280 (1998)
18. Chandra, A.K., Nguyen, M.T., Zeegers-Huyskes, T.: Theoretical study of the interaction thymine and water. Protonation and deprotonation enthalpies and comparison with uracil. J. Phys. Chem. A **102**, 6010–6016 (1998)

19. Chandra, A.K., Nguyen, M.T., Uchimaru, T., Zeegers-Huyskes, T.: Protonation and deprotonation enthalpies of guanine and adenine and implications for the structure and energy of their complexes with water: comparison with uracil, thymine, and cytosine. J. Phys. Chem. A **103**, 8853–8860 (1999)
20. Kurinovich, M.A., Lee, J.K.: The acidity of uracil from the gas phase to solution: the coalescence of the N1 and N3 sites and implications for biological glycosylation. J. Am. Chem. Soc. **122**, 6258–6262 (2000)
21. Kryachko, E., Nguyen, M.T., Zeegers-Huyskes, T.: Thiouracils: acidity, basicity, and interaction with water. J. Phys. Chem. A **105**, 3379–3387 (2001)
22. Kryachko, E., Nguyen, M.T., Zeegers-Huyskes, T.: Density functional calculations on protonated and deprotonated thiouracils and their complexes with water. Chem. Phys. **264**, 21–35 (2001)
23. Chandra, A.K., Nguyen, M.T., Zeegers-Huyskes, T.: Theoretical study of protonation and deprotonation cytosine. Implications for interaction of cytosine with water. J. Mol. Struct. **519**, 1–11 (2000)
24. Kryachko, E., Nguyen, M.T., Zeegers-Huyskes, T.: Theoretical study of tautomeric forms of uracil. 1. Relative order of stabilities and their relation to proton affinities and deprotonation enthalpies. J. Phys. Chem. **105**, 1288–1295 (2001)
25. Kryachko, E., Nguyen, M.T., Zeegers-Huyskes, T.: Theoretic study of uracil tautomers. 2. Interaction with water. J. Phys. Chem. A **105**, 1934–1943 (2001)
26. Chandra, A.K., Uchimaru, T., Zeegers-Huyskes, T.: Theoretical study on protonated and deprotonated 5-substituted uracil derivatives and their complexes with water. J. Mol. Struct. **605**, 213–220 (2002)
27. Kurinovich, M.A., Lee, J.K.: The acidity of uracil and uracil analogs in the gas phase: four surprisingly acidic sites and biological implications. J. Am. Soc. Mass Spectrom. **13**, 985–995 (2002)
28. Huang, Y., Kenttämaa, H.: Theoretical estimation of the 298 K gas-phase acidities of the pyrimidine-based nucleobases uracil, thymine, and cytosine. J. Phys. Chem. A **107**, 4893–4897 (2003)
29. Di Laudo, M., Whittleton, S.R., Wetmore, S.D.: Effects of hydrogen bonding on the acidity of uracil. J. Phys. Chem. A **107**, 10406–10413 (2003)
30. Whittleton, S.R., Hunter, K.C., Wetmore, S.D.: Effects of hydrogen bonding on the acidity of uracil derivatives. J. Phys. Chem. A **108**, 7709–7718 (2004)
31. Miller, T.M., Arnold, S.T., Viggiano, A.A., Miller, A.E.S.: Acidity of a nucleotide base: uracil. J. Phys. Chem. A **108**, 3439–3446 (2004)
32. Sharma, S., Lee, J.K.: Acidity of adenine and adenine derivatives and biological implications. A computational and experimental gas-phase study. J. Org. Chem. **67**, 8360–8365 (2002)
33. Sharma, S., Lee, J.K.: Gas-phase acidity studies of multiple sites of adenine and adenine derivatives. J. Org. Chem. **69**, 7018–7025 (2004)
34. Hunter, K.C., Rutledge, L.R., Wetmore, S.D.: The hydrogen bonding properties of cytosine: a computational study of cytosine complexed with hydrogen fluoride, water, and ammonia. J. Phys. Chem. A **109**, 9554–9562 (2005)
35. Lamsabhi, A.M., Alcami, M., Mó, O., Yáñez, M.: Gas-phase deprotonation of uracil-Cu^{2+} and thiouracil-Cu^{2+} complexes. J. Phys. Chem. A **110**, 1943–1950 (2006)
36. Bennett, M.T., Rodgers, M.T., Hebert, A.S., Ruslander, L.E., Eisele, L., Drohat, A.C.: Specificity of human thymine DNA glycosylase depends on *N*-glycosidic bond stability. J. Am. Chem. Soc. **128**, 12510–12519 (2006)
37. Chen, E.C.M., Herder, C., Chen, E.S.: The experimental and theoretical gas phase acidities of adenine, quinine, cytosine, uracil, thymine, and halouracils. J. Mol. Struct. **798**, 126–133 (2006)
38. Sun, X., Lee, J.K.: Acidity and proton affinity of hypoxanthine in the gas phase versus in solution: intrinsic reactivity and biological implications. J. Org. Chem. **72**, 6548–6555 (2007)
39. Liu, M., Li, T., Amegayibor, F.S., Cardoso, D.S., Fu, Y., Lee, J.: Gas-phase thermochemical properties of pyrimidine nucleobases. J. Org. Chem. **73**, 9283–9291 (2008)
40. Zhachkina, A., Lee, J.K.: Uracil and thymine reactivity in the gas phase: the S_N2 reaction and implications for electron delocalization in leaving groups. J. Am. Chem. Soc. **131**, 18376–18385 (2009)
41. Zhachkina, A., Liu, M., Sun, X., Amegayibor, F.S., Lee, J.K.: Gas-phase thermochemical properties of the damaged base O^6-methylguanine versus adenine and guanine. J. Org. Chem. **74**, 7429–7440 (2009)
42. Bachrach, S.M., Dzierlenga, M.W.: Microsolvation of uracil and its conjugate bases: a DFT study of the role of solvation on acidity. J. Phys. Chem. A **115**, 5674–5683 (2011)
43. Kimura, E., Kitamura, H., Koike, T., Shiro, M.: Facile and selective electrostatic stabilization of uracil $N(1)^-$ anion by a proximate protonated amine: a chemical implication for why uracil N(1) is chosen for glycosylation site. J. Am. Chem. Soc. **119**, 10909–10919 (1997)
44. Stivers, J.T., Jiang, Y.L.: A mechanistic perspective on the chemistry of DNA repair glycosylases. Chem. Rev. **103**, 2729–2759 (2003)
45. Wincel, H.: Microhydration of protonated nucleic acid bases and protonated nucleosides in the gas phase. J. Am. Soc. Mass Spectrom. **20**, 1900–1905 (2009)
46. Wincel, H.: Gas-phase hydration thermochemistry of sodiated and potassiated nucleic acid bases. J. Am. Soc. Mass Spectrom. **23**, 1479–1487 (2012)
47. Wincel, H.: Hydration energies of protonated and sodiated thiouracils. J. Am. Soc. Mass Spectrom. **25**, 2134–2142 (2014)
48. Longley, D.B., Harkin, D.P., Johnston, P.G.: 5-Fluorouracil: mechanisms of action and clinical strategies. Nat. Rev. **3**, 330–338 (2003)
49. Parker, J.B., Stivers, J.T.: Dynamics of uracil and 5-fluorouracil in DNA. Biochemistry **50**, 612–617 (2011)
50. Saenger, W.: Principles of Nucleic Acid Structure, pp. 159–200. Springer, New York (1984)
51. Miller, W.H., Robin, R.O., Astwood, E.B.: Studies in chemotherapy. XI. Oxidation of 2-thiouracil and related compound. J. Am. Chem. Soc. **67**, 2201–2204 (1945)
52. Sulkowska, A., Równicka, J., Bojko, B., Sulkowski, W.: Interaction of anticancer drugs with human and bovine serum albumin. J. Mol. Struct. **651**, 133–140 (2003)
53. Wincel, H.: Hydration of gas-phase protonated alkylamines, amino acids and dipeptides produced by electrospray. Int. J. Mass Spectrom. **251**, 23–31 (2006)
54. Caldwell, G., Kebarle, P.: Binding energies and structural effects in halide anion- ROH and RCOOH complexes from gas-phase equilibria measurements. J. Am. Chem. Soc. **106**, 967–969 (1984)
55. Kebarle, P.: A brief overview of the present status of the mechanism involved in electrospray mas spectrometry. J. Mass Spectrom. **35**, 804–817 (2000)
56. Shapiro, R., Kang, S.: Uncatalyzed hydrolysis of deoxyuridine, thymidine, and 5-bromodeoxyuridine. Biochemistry **8**, 1806–1810 (1969)
57. Psoda, A., Schugar, D.: Structure and tautemerism of the neutral and monoanionic forms of 2-thiouracil, 2,4-dithiouracil and their nucleosides, and some related derivatives. Acta Biochim. Pol. **26**, 55–72 (1979)
58. Wempen, I.: Spectrophotometric studies of nucleic acid derivatives and related compounds. VI. On the structure of certain 5- and 6-halogenouracils and -cytosines. J. Am. Chem. Soc. **86**, 2474–2477 (1964)
59. IIich, P., Hemann, C.F., Hille, R.: Molecular vibrations of solvated uracil. Ab initio reaction field calculations and experiment. J. Phys. Chem. B **101**, 10923–10938 (1997)
60. Abdrahkimova, G.S., Ovcchinnikov, M.Y., Lobov, A.L., Spirikhin, L.V., Ivanov, S.P., Khursan, S.L.: 5-Fluorouracil solutions: NMR study of acid-base equilibrium in water and DMSO. J. Phys. Org. Chem. **27**, 876–883 (2014)
61. Cole, C.A., Wang, Z.W., Snow, T.P., Bierbaum, V.M.: Anionic derivatives of uracil: fragmentation and reactivity. Phys. Chem. Chem. Phys. **16**, 17835–17844 (2014)
62. Plützer, C., Kleinermans, K.: Tautomers and electronic states of jet-cooled adenine investigated by double resonance spectroscopy. Phys. Chem. Chem. Phys. **4**, 4877–4882 (2002)
63. Kim, H.-S., Ahn, D.-S., Chung, S.-Y., Kim, S.-K., Lee, S.: Tautomerization of adenine facilitated by water: computational study by microsolvation. J. Phys. Chem. A **111**, 8007–8012 (2007)
64. Huang, R., Zhao, L.-B., Wu, D.-Y., Tian, Z.-Q.: Tautomerization, solvent effect, and binding interaction on vibrational spectra of adenine-Ag^+ complexes on silver surfaces: a DFT study. J. Phys. Chem. C **115**, 13739–13750 (2011)
65. Dreyfus, M., Dodin, G., Bensaude, O., Dubois, J.E.: Tautomerism of purines. I. N(7)H<=>N(9)H equilibrium in adenine. J. Am. Chem. Soc. **97**, 2369–2376 (1975)
66. Gonnella, N.C., Nakanishi, H., Holwick, J.B., Horowitz, D.S., Kanamori, K., Leonard, N.J., Roberts, J.D.: Studies of tautomers and protonation of adenine and its derivatives by nitrogen-15 nuclear magnetic resonance spectroscopy. J. Am. Chem. Soc. **105**, 2050–2055 (1983)
67. Cohen, B., Hare, P.M., Kohler, B.: Ultrafast excited-state dynamics of adenine and monomethylated adenines in solution: implications for the nonradiative decay mechanism. J. Am. Chem. Soc. **125**, 13594–13601 (2003)

68. Aidas, K., Mikkelsen, K.V., Kongsted, J.: On the existence of the H3 tautomer of adenine in aqueous solution. Rationalizations based on hybrid quantum mechanics/molecular mechanics predictions. Phys. Chem. Chem. Phys. **12**, 761–768 (2010)
69. Stachowicz-Kuśnierz, A., Korchowiec, J.: Nucleophilic properties of purine bases: ingerent reactivity versus reaction conditions. Struct. Chem. **27**, 543–555 (2016)
70. Shukla, M.K., Leszczynski, J.: A DFT investigation on effects of hydration on the tautomeric equilibria of hypoxanthine. J. Mol. Struct. **529**, 99–112 (2000)
71. Costas, M.E., Acevedo-Chávez, R.: Density functional study of the neutral hypoxanthine tautomeric forms. J. Phys. Chem. A **101**, 8309–8318 (1997)
72. Lin, J., Yu, C., Peng, S., Akiyama, I., Li, K., Lee, L.K., LeBreton, P.R.: Ultraviolet photoelectron studies of the ground-state electronic structure and gas-phase tautomerism of hypoxanthine and guanine. J. Phys. Chem. **84**, 1006–1012 (1980)
73. San Román-Zimbrón, M.L., Costas, M.E., Acevedo-Chávez, R.: Neutral hypoxanthine in aqueous solution: quantum chemical and Monte-Carlo studies. J. Mol. Struct. (THEOCHEM) **711**, 83–94 (2004)
74. Gogia, S., Jain, A., Puranik, M.: Structures, ionization equilibria, and tautomerism of 6-oxopurines in solution. J. Phys. Chem. B **111**, 15101–15118 (2009)
75. Puzzarini, C., Biczysko, M.: Microhydration of 2-thiouracil: Molecular structure and spectroscopic parameters of the thiouracil–water complex. J. Phys. Chem. A **119**, 5386–5395 (2015)
76. Pan, S., Verhoeven, K., Lee, J.K.: Investigation of the initial fragmentation of oligodeoxy-nucleotides in quadrupole ion trap: charge level-related base loss. J. Am. Soc. Mass Spectrom. **16**, 1853–1865 (2005)